

10-2009

Determination of Size Effects during the Phase Transition of a Nanoscale Au-Si Eutectic

B.J. Kim

Purdue University - Main Campus

J Tersoff

IBM Corp.

C Y. Wen

Purdue University - Main Campus

M.C. Reuter

IBM Corp.

E A. Stach

Birck Nanotechnology Center and School of Materials Engineering, Purdue University, eastach@purdue.edu

See next page for additional authors

Follow this and additional works at: <http://docs.lib.purdue.edu/nanopub>



Part of the [Nanoscience and Nanotechnology Commons](#)

Kim, B.J.; Tersoff, J.; Wen, C.Y.; Reuter, M.C.; Stach, E.A.; and Ross, F.M., "Determination of Size Effects during the Phase Transition of a Nanoscale Au-Si Eutectic" (2009). *Birck and NCN Publications*. Paper 570.

<http://docs.lib.purdue.edu/nanopub/570>

This document has been made available through Purdue e-Pubs, a service of the Purdue University Libraries. Please contact epubs@purdue.edu for additional information.

Authors

B J. Kim, J Tersoff, C Y. Wen, M C. Reuter, E A. Stach, and F M. Ross

Determination of Size Effects during the Phase Transition of a Nanoscale Au-Si Eutectic

B. J. Kim,¹ J. Tersoff,² C.-Y. Wen,¹ M. C. Reuter,² E. A. Stach,¹ and F. M. Ross²

¹*School of Materials Engineering and Birck Nanotechnology Center, Purdue University, West Lafayette, Indiana 47907, USA*

²*IBM Research Division, T. J. Watson Research Center, Yorktown Heights, New York 10598, USA*

(Received 5 August 2009; published 6 October 2009)

The phase diagram of a nanoscale system can be substantially different than in the bulk, but quantitative measurements have proven elusive. Here we use *in situ* microscopy to observe a phase transition in a nanoscale system, together with a simple quantitative model to extract the size effects from these measurements. We expose a Au particle to disilane gas, and observe the transition from a two-phase Au + AuSi system to single-phase AuSi. Size effects are evident in the nonlinear disappearance of the solid Au. Our analysis shows a substantial shift in the liquidus line, and a discontinuous change in the liquid composition at the transition. It also lets us estimate the liquid-solid interfacial free energy.

DOI: 10.1103/PhysRevLett.103.155701

PACS numbers: 64.60.Q-, 82.60.Qr

The increasing focus on nanoscale physics and its applications has led to intense interest in understanding how the phase diagrams of alloys change with decreasing system size [1–4]. This problem has received particular attention in the context of vapor-liquid-solid growth of nanowires [2–4], where the wire serves as a nonbulk reservoir for one component [5]. An even more fundamental problem is the equilibrium phase diagram of a small closed system, i.e., one with a fixed amount of material rather than a reservoir [1,4]. Both problems have been addressed theoretically [1–4]. Yet to date there are few experimental results [6,7], and none allowing direct comparison with the predictions of theory.

Here we present experimental measurements of the phase transition in a closed [8] nanoscale system—the classic eutectic system Au + Si. Beginning with Au nanoparticles ~35 nm in diameter, we add Si continuously and observe the transition from two-phase Au + AuSi to single-phase AuSi. The Au crystal shrinks smoothly with time until it is roughly 15 nm in diameter. At that point it shrinks more rapidly and vanishes, suggesting a strong size effect.

We derive a simple model for the behavior, based on the same physics as in earlier theoretical work [1,4]. The model parameters are determined by fitting the experimental data. From the model and fitted parameters, we then calculate the size-related change in the phase diagram. We find a substantial shift in the liquidus line, lowering the transition temperature by ~240 °C. In addition, the nature of the phase transition is different than in the bulk: there is an activation barrier for the transition from two-phase to single phase, and a discontinuous change in the equilibrium liquid composition at the liquidus. Most intriguingly, the measurement allows us to estimate the free energy of the liquid-solid interface, which is crucial for nucleation but which is extremely difficult to measure directly. Discussions of size effects usually focus on the role of surface energy [9]; but here the dependence of liquid

composition on the size of the solid due to finite liquid volume also plays a crucial role.

We begin with Au particles deposited from an aerosol source [10] onto silicon nitride covered Si wafers [11]. These particles were imaged in an ultrahigh vacuum transmission electron microscope during simultaneous heating and exposure to disilane. Details of the experimental setup [12,13] and temperature calibration [14] are given elsewhere. As disilane dissociates on the particle surface, the added Si combines with the Au to form a liquid AuSi eutectic. The amount of solid Au remaining is measured as a function of time from videos recorded using dark-field imaging conditions.

The evolution of our Au + Si system is shown in side view in Fig. 1. The first four frames were recorded at an orientation where the crystalline Au lattice provides bright

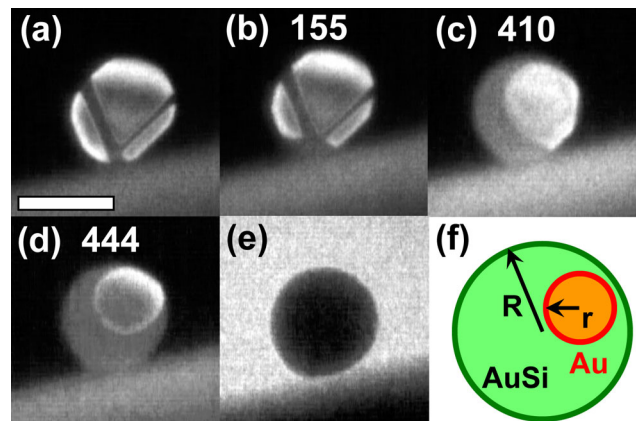


FIG. 1 (color online). (a)–(d) Dark-field images in side view during the solid to liquid transformation at 525 °C and 1.5×10^{-6} Torr disilane, with time in seconds. The scale bar is 30 nm. The substrate appears as a nearly horizontal band at the bottom of each image. (e) Bright field image showing the droplet after the transformation is complete. (f) Idealized schematic of the inferred geometry.

contrast [15]. The Au particle appears to consist of a single crystal with multiple twins (visible as dark bands), and the amount of solid Au decreases with time. Figure 1(e) shows the liquid droplet that remains after the crystal has disappeared. Together with images in plan view (not shown), Fig. 1 gives a good picture of the 3D geometry. The crystal shrinks roughly as a solid sphere inside a liquid sphere, as illustrated in Fig. 1(f). Thus we can estimate volume and interface area with reasonable accuracy.

The liquid appears to form initially as a shell around the solid Au. This suggests that AuSi wets Au, so that the surface exposed to disilane is liquid from an early time [16]. Indeed, as shown in Figs. 2(a) and 2(b), the Au starts to shrink almost immediately after disilane is introduced at time $t = 0$.

Since Si is added continuously, we would expect the volume of the Au crystal to shrink roughly linearly with time. The crystal size vs time is plotted in Fig. 2 for reactions at 500 °C and 525 °C. In both cases, the crystal volume decreases nearly linearly with time as expected, until $r^3 \lesssim 500 \text{ nm}^3$ ($r \lesssim 8 \text{ nm}$). At that point the solid shrinks rapidly and disappears [15].

This behavior presumably originates in the increasing chemical potential of the Au solid as it shrinks (analogous to the Gibbs-Thomson pressure), which destabilizes a very small particle [9]. To quantify and test this interpretation, we derive a simple model to describe the evolution. For our purposes we can neglect the tiny mutual solubilities of Au and Si in the solid phase, as well as the slight difference in molar volume between the Au solid and AuSi liquid. Then for a sphere within a sphere, we can write the free energy of our Au + AuSi system as

$$F = \frac{2\pi}{3}(R^3 - \rho^3)(c_l - c_b)^2 g'' + 4\pi\rho^2\gamma_{ls} + 4\pi R^2\gamma_{vl}. \quad (1)$$

Here our thermodynamic reference states are solid Au and liquid AuSi at the bulk liquidus composition; ρ is the radius of the Au solid; R is the radius of the total system; and γ_{ls} and γ_{vl} are the liquid-solid and vapor-liquid interface energies. The composition (Au fraction) c of our system is thus $c = R_0^3/R^3$ where R_0 describes the total volume ($4\pi/3R_0^3$) of Au (which is present from the beginning and remains constant), and the amount of Si is $V_{Si} = (4\pi/3)(R^3 - R_0^3)$. The composition c_l of the liquid is $c_l = (R_0^3 - \rho^3)/(R^3 - \rho^3)$. Since we are interested in liquid compositions not too far from the bulk liquidus c_b , we have expanded $g(c_l)$ to second order in $c_l - c_b$, as $g(c_l) \approx (c_l - c_b)^2 g''/2$, where $g'' = d^2g/dc^2$ is evaluated at c_b .

The resulting dependence of free energy F on the size ρ of the solid Au is illustrated in Fig. 3(a). (The choice of parameter values is explained below; for now we focus on the generic aspects of the behavior.) The total amount of Au (R_0) is fixed, and each curve shows a different amount of Si, i.e., a different R and c . For low Au fraction (top two curves) the energy increases monotonically with ρ , so any

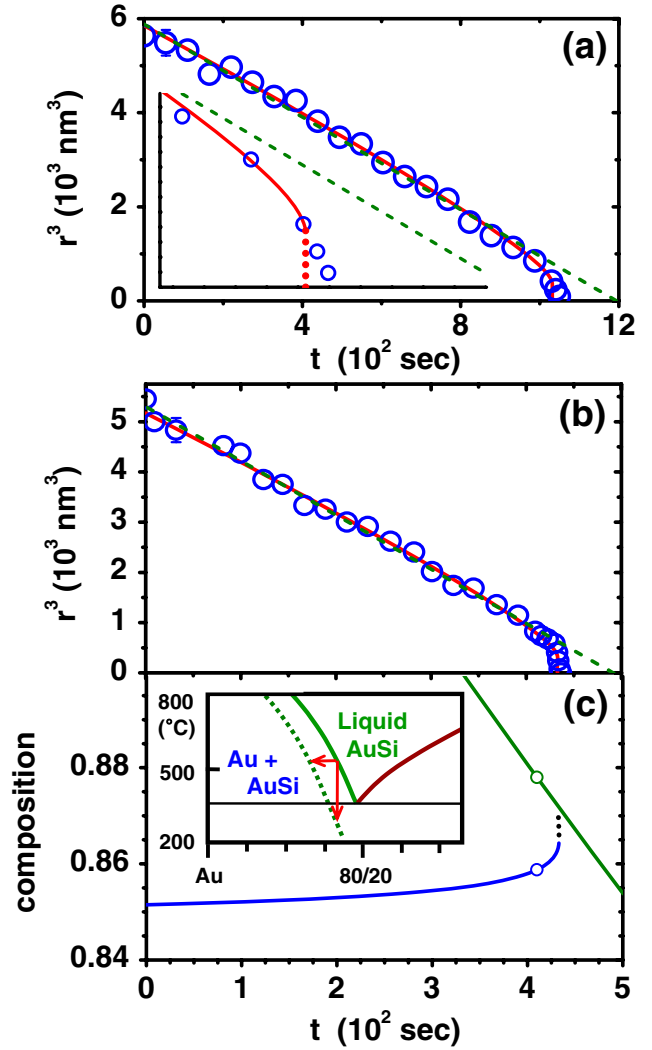


FIG. 2 (color online). (a) Size r^3 of solid Au, vs time t after introducing 1.5×10^{-6} Torr disilane at 500 °C. Straight dashed line (dark green) is a least-square fit excluding the final stage of more rapid shrinking (last 4 data points). Curved line (red) is Eq. (3) with $k = 619 \text{ nm}/(\text{Torr s})$ and $\eta = 0.165 \text{ nm}$. Inset (lower left) shows expanded view of final stage, with dotted vertical line indicating stability limit. (b) Same as (a) for a different particle at 525 °C. Curved line (red) is Eq. (3) with $k = 1351 \text{ nm}/(\text{Torr s})$ and $\eta = 0.146 \text{ nm}$. (c) Composition vs time for same particle as (b), calculated using fitted parameters. Upper line (dark green) is the total composition of the system [from Eq. (3) as described in text]. Lower curve (blue) is liquid composition from Eq. (4). Dotted vertical line shows stability limit. Circles on upper and lower curve indicate, respectively, the liquidus composition and the composition of the liquid in the two-phase system at the liquidus. Inset shows relevant portion of phase diagram with calculated shift in liquidus composition, illustrating the corresponding reduction expected for transition temperature.

solid Au is unstable and the system will be a single-phase liquid. At high Au fraction (bottom two curves) the energy increases to a maximum with increasing ρ , and then decreases to a minimum. This minimum corresponds to the

stable Au particle that we observe experimentally, and we use r to denote this size, i.e., the value of ρ at which $dF/d\rho = 0$. The maximum corresponds to the “critical size,” the transition state between single-phase and two-phase systems.

Intermediate compositions show the same general behavior (middle two curves). However, in this case the minimum at nonzero ρ has higher free energy than the single-phase liquid (where $\rho = 0$). Thus solid Au is absent in equilibrium, but can be present as a metastable particle. The liquidus of the nanoscale system is the equilibrium boundary between single phase and two phase, i.e., the composition dividing stable and metastable regimes.

Physically, V_{Si} is the independent variable. However, it is convenient to instead calculate the value of R (and thus V_{Si} and c_l as given above) for a given r . From Eq. (1) we solve $dF/d\rho = 0$ to lowest nontrivial order in $c_l - c_b \ll 1$. This gives

$$R^3 = R_0^3 + (R_0^3 - r^3) \left[\left(\frac{\eta}{r} + c_b \right)^{-1} - 1 \right], \quad (2)$$

where $\eta = 2\gamma_{\text{ls}}/[g''(1 - c_b)]$. For $\eta = 0$, this reduces to the bulk behavior.

This is illustrated in Fig. 3(b) for several different initial Au sizes R_0 . For each value of r we calculate the corresponding R and from that c . We see that for any c there are either zero or two values at which $dF/d\rho = 0$. In comparing with experiment we want the upper solution, which corresponds to the stable (or metastable) size of solid Au in the two-phase system.

As Si is added and c decreases, Fig. 3(b) shows that the Au particle shrinks increasingly rapidly until the point where dr/dc diverges. At this point, the Au particle becomes unstable, so the size r is a discontinuous function of c . Actually, at any composition below the liquidus the Au is metastable and could disappear, if it overcomes the activation barrier. The liquidus is indicated by a dot on each curve in Fig. 3(b). The metastable range of composition (to the right of the dot) is seen to decrease with increasing system size, vanishing in the bulk. Thus the metastable solid is strictly a finite-size effect.

In our experiment, we do not measure composition directly; we measure r vs time t rather than composition c . Fortunately the kinetics of our system are well understood [16,17], allowing us to recast the model in an appropriate form. We turn on the disilane flow at time $t = 0$, and the Au is almost immediately wetted with AuSi, after which the amount of Si increases at a rate proportional to the surface area [17]. Thus $\frac{d}{dt}(\frac{4}{3}\pi R^3) = kP(4\pi R^2)$, giving $R = kPt + R_0$, where P is the nominal disilane pressure and k is a rate constant. Then from Eq. (2),

$$kPt = \left(\left[\frac{1}{\eta r^{-1} + c_b} - 1 \right] (R_0^3 - r^3) + R_0^3 \right)^{1/3} - R_0. \quad (3)$$

The curved lines in Fig. 2 show Eq. (3). The values of k and η are fitted directly to the experimental data. Fitting in

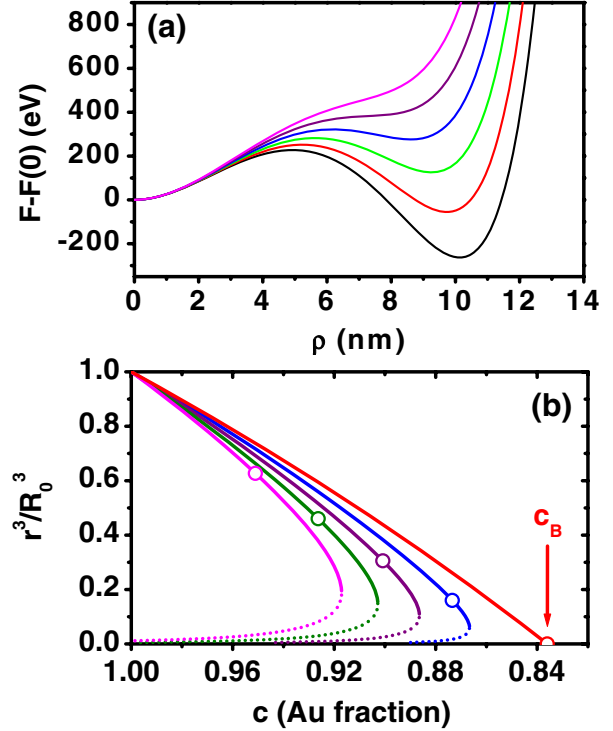


FIG. 3 (color online). (a) Free energy F (relative to the single-phase liquid) vs Au size ρ . Parameters are for 500 °C as in Fig. 2(a), see text for details. Curves from bottom to top are, respectively, for compositions $c = 0.876, 0.874, 0.872, 0.870, 0.868, \text{ and } 0.866$. (b) Au particle size vs composition for different system sizes, from Eq. (2) with parameters of Fig. 2(a) as described in text. Rightmost curve (nearly straight, red) is for bulk, $R_0 \rightarrow \infty$; second from right (blue) is for actual size, $R_0 = 18$ nm; and subsequent curves are for $R_0 = 9, 6, \text{ and } 4.5$ nm, respectively. Circles indicate liquidus composition, c_b is the bulk liquidus, and the rightmost point of each curve is the metastability limit.

this way implicitly assumes (i) that the kinetics are fast enough for the Au size ρ to remain near its stationary value r as the composition evolves; and (ii) that the metastable Au particle survives for tens of seconds, until close to the composition at which it becomes unstable. The justification for assumption (ii) is discussed below.

The data are fitted well with the two parameters k and η , supporting the model developed above. We can use the fitted model to further quantify the size effects. We find that at 500–525 °C the liquidus is shifted to a composition 3.5% more Au-rich than in the bulk. This implies that for a system at the bulk liquidus composition, size effects lower the transition temperature by ~ 240 °C, as illustrated in the inset in Fig. 2(c).

We can also calculate the composition of the liquid,

$$c_l = \frac{R_0^3 - r^3}{(kPt + R_0)^3 - r^3}. \quad (4)$$

This is shown in Fig. 2(c), together with the composition of the total system. In a bulk system, the liquid composition

remains constant at the bulk liquidus value until the solid has disappeared, at which point the liquid composition begins to vary. There is no discontinuity in composition at the transition. In contrast, we see that in the nanoscale system there is substantial variation in the liquid composition, with the liquid's Au fraction increasing as the Au solid shrinks. In equilibrium, the liquid composition jumps discontinuously at the liquidus in going from the two-phase to the single-phase system. In our experiment, where the solid persists to near the instability point, the jump in c_l is smaller but still quite significant, as seen in Fig. 2(c).

To see how these size effects scale with system size, we solve Eq. (2) for $dR/dr \rightarrow 0$ to get r at the instability point. Substituting this back into Eq. (2) gives the shift in liquidus composition: $\Delta c \approx 4c_b^{1/4}(1 - c_b)^{1/4}(\eta/3R_0)^{3/4}$, to lowest order in η . Thus as the system size increases, or η decreases, this size effect decreases as $(\eta/R_0)^{3/4}$ or volume^{1/4} [1].

Interfacial energies are crucial in many processes, including nucleation and nanowire growth; but they are extremely difficult to measure. We have determined η , which equals $2\gamma_{ls}/[(1 - c_b)g'']$, and we can calculate g'' using published thermodynamic models of the AuSi alloy [18]. In this way we find $\gamma_{ls} \approx 2.0$ eV/nm² or 0.3 J/m² at 525 °C. This is a small interfacial energy—more than a factor of 2 smaller than the value quoted in Ref. [2] for the γ_{ls} between Si and AuSi. Such a small γ could explain why we see a nearly spherical Au particle surrounded by liquid, if the Au-AuSi energy is relatively small compared to Au-vapor or Au-substrate interfacial energies.

Given γ_{ls} as well as g'' , we can put the results of Fig. 3(a) on an absolute energy scale as shown. We see that near the liquidus there is a prohibitive energy barrier of well over 200 eV for the Au to disappear. This barrier decreases smoothly with composition, going to zero at the instability point. Moreover, the small system volume gives an unusually small transition-state entropy, further impeding the transition. This supports our assumption that the metastable Au survives until relatively close to the point where it becomes unstable.

If we continue adding Si, eventually solid Si nucleates from the AuSi liquid. That case was studied previously, and no observable size effects were found [16]. The value of γ_{ls} is of course different for Si vs Au in AuSi. More importantly, the geometry is very different—Si in AuSi had interfaces with the vapor and substrate as well as with the liquid, making it unsurprising that the size effects would be very different.

In conclusion, by combining quantitative *in situ* measurements with theoretical modeling, we study the phase diagram and related properties of a nanoscale system. At easily attainable sizes there are substantial shifts in the

liquidus line composition and transition temperature. We note several features that are absent in the bulk, including metastability of the two-phase system, and a discontinuous change in liquid composition at the transition. Such effects need to be considered when examining phase transformations in nanoscale systems.

We gratefully acknowledge E. J. Schwalbach and P. W. Voorhees for helpful discussions, and K. A. Dick for providing the aerosol particles. This work was partially funded by NSF under Grants No. DMR 0606395 and DMR 0907483.

-
- [1] J. Weissmüller, P. Bunzel, and G. Wilde, *Scr. Mater.* **51**, 813 (2004).
 - [2] S. M. Roper, S. H. Davis, S. A. Norris, A. A. Golovin, P. W. Voorhees, and M. Weiss, *J. Appl. Phys.* **102**, 034304 (2007).
 - [3] H. Adhikari, A. F. Marshall, I. A. Goldthorpe, C. E. D. Chidsey, and P. C. McIntyre, *ACS Nano* **1**, 415 (2007); H. Adhikari, P. C. McIntyre, A. F. Marshall, and C. E. D. Chidsey, *J. Appl. Phys.* **102**, 094311 (2007).
 - [4] E. J. Schwalbach and P. W. Voorhees, *Nano Lett.* **8**, 3739 (2008).
 - [5] E. I. Givargizov, *J. Cryst. Growth* **31**, 20 (1975).
 - [6] E. Sutter and P. Sutter, *Nano Lett.* **8**, 411 (2008).
 - [7] J. G. Lee, H. Mori, and H. Yasuda, *Phys. Rev. B* **65**, 132106 (2002).
 - [8] Although we are adding Si, the system is closed in the sense that at any moment its composition is fixed—the system cannot change its composition by exchanging material with a reservoir.
 - [9] J. W. Christian, *The Theory of Transformations in Metals and Alloys* (Pergamon, Oxford, 2002).
 - [10] M. H. Magnusson *et al.*, *J. Nanopart. Res.* **1**, 243 (1999).
 - [11] For plan view observations, 80 nm thick amorphous silicon nitride membranes were created on 200 μm thick Si specimens by etching from the back side, and aerosols deposited at a density of 1 μm^{-2} were imaged through the membrane. For side view observations, aerosols were deposited onto a diced unthinned silicon nitride coated wafer, which was imaged with the electron beam parallel to the aerosol-covered surface.
 - [12] M. Hammar, F. K. LeGoues, J. Tersoff, M. C. Reuter, and R. M. Tromp, *Surf. Sci.* **349**, 129 (1996).
 - [13] F. M. Ross, J. Tersoff, and M. C. Reuter, *Phys. Rev. Lett.* **95**, 146104 (2005).
 - [14] E. A. Stach *et al.*, *J. Appl. Phys.* **83**, 1931 (1998).
 - [15] Bright field images [not shown] confirm that the sudden shrinkage near the end is not a dark-field artifact caused by rotation of the remaining Au crystal.
 - [16] B. J. Kim *et al.*, *Science* **322**, 1070 (2008).
 - [17] S. Kodambaka, J. Tersoff, M. C. Reuter, and F. M. Ross, *Phys. Rev. Lett.* **96**, 096105 (2006).
 - [18] P. Y. Chevalier, *Thermochim. Acta* **141**, 217 (1989).